Fuel 375 (2024) 132566

Contents lists available at ScienceDirect

Fuel

journal homepage: www.elsevier.com/locate/fuel

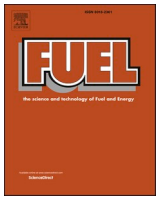

Full Length Article

Influence of micro-aeration in the production of volatile fatty acids (VFA) from wastewaters with high salinity

M. Salomé Duarte [a,b,1,*], Ricardo J.C. Fernandes [a,c,1], João Sousa [a], Carla Pereira [a], Daniela P. Mesquita [a,b], M. Madalena Alves [a,b]

[a] CEB – Centre of Biological Engineering, University of Minho, Campus de Gualtar, 4710-057 Braga, Portugal
[b] LABBELS – Associate Laboratory, Braga/Guimarães, Portugal
[c] Physics Centre of Minho and Porto Universities (CF-UM-UP), University of Minho, Campus de Gualtar, 4710-057 Braga, Portugal

ARTICLE INFO

Keywords:
Anoxic
Microaerophilic
Acidogenesis
Image analysis

ABSTRACT

Waste management and valorization are seen as pivotal drivers for adopting a circular economy. The production of volatile fatty acids (VFA) through anaerobic digestion (AD) fits perfectly into these emerging social and industrial dynamics, being the VFA considered valuable products, namely in chemical industries. Therefore, this work focuses on VFA production through AD, using wastes and wastewaters, with high salinity content (20 g/L) in continuous bioreactors. The effect of micro-aeration during acidogenesis of high-salinity wastes/wastewaters was accessed for more than 500 days, divided in 5 main periods, by analysing different physicochemical parameters like oxidation–reduction potential (ORP), salinity, pH, COD, and VFA profile. Sludge properties were also analysed through quantitative image analysis (QIA) and integrating Principal Component Analysis (PCA). The results demonstrate that the high salinity does not appear as a limiting factor, with soluble COD (30 g/L) being constant through operation time in both reactors, as well as VFA/sCOD ratio (60 % – 80 %). Due to micro-aeration, differences between anoxic (R1) and microaerophilic (R2) reactors were observed, with the second one presenting lower value of ORP in some periods during the assay. This indicates the presence of aerobic or facultative microorganisms, which have consumed oxygen. Also, higher concentrations of hexanoate in the microaerophilic reactor (R2) were obtained in those periods. The application of QIA combined with PCA has revealed that micro-aeration significantly impacts the morphology and size of aggregates.

1. Introduction

Waste management is considered one of the biggest environmental concerns [1]. With the increase of the worldwide population, and with all the negative consequences that this uncontrolled growth leads to, new efforts have to be done to develop new technologies and processes that can mitigate waste accumulation in different environments. The valorization of waste is, perhaps, the one that makes more sense for today's society [1,2]. The constant search for adopting a circular economy in the urban and industrial ecosystems can be a turning point in waste management, especially by using these wastes to create new economically viable processes and products, helping not only the environment, but also societies in general. Food waste (FW) and agro-food wastewaters (WW) are considered top priorities on this subject, since their generation is increasing with the growth of worldwide population, being a huge challenge [3,4]. It has been estimated that 2.2 billion tons of FW will be generated by 2025, ending up in soils, air and water systems, and that by 2050, 70 % of the worldwide population will face energy, food and water challenges [4,5].

One of the highly valuable products that can be generated in waste valorisation through anaerobic processes (AD) are volatile fatty acids (VFA). They have recently attracted a lot of attention, being widely explored for a wide range of applications such as building blocks in chemical industries, as well as in the pharmaceutical and tanning sectors [6,7]. They represent a high economic value, first due to the widespread possible applications, but also due to the possibility of obtaining VFA through waste/wastewater fermentation. Castro-Fernandez *et al.* assessed the economic value of VFA production from food waste, achieving values of 22.9 €/t FW, higher than the obtained from biomethane (11.7 €/t FW) [8] The production of VFA through AD of

* Corresponding author at: CEB – Centre of Biological Engineering, University of Minho, Campus de Gualtar, 4710-057 Braga, Portugal.
E-mail address: salomeduarte@ceb.uminho.pt (M. Salomé Duarte).
[1] Contributed equally to this work.

https://doi.org/10.1016/j.fuel.2024.132566
Received 26 March 2024; Received in revised form 22 June 2024; Accepted 16 July 2024
Available online 24 July 2024

residues can also lower production costs, making it more suitable for large-scale production processes, also integrating a circular economy [9]. The AD process occurs in four different steps: hydrolysis, acidogenesis, acetogenesis and methanogenesis. VFA formation, as the name says, is formed in the second step, acidogenesis [10]. To promote VFA production through AD, is important to promote both hydrolysis and acidogenesis, while inhibiting methanogenesis [11]. Parameters such as pH, organic loading rate (OLR), retention time, salinity content, reactor configuration, can influence bacteria behaviour and, consequently, inhibit or promote steps in AD. One of those parameters that have been considered to affect greatly this process is salinity, promoting the formation and accumulation of VFA [12]. Anaerobic microorganisms are very sensitive to saline conditions, mostly due to cell dehydration which, therefore, leads to cell demise [9]. The most sensitive organisms, the ones with a less known capacity to adapt and acclimate under these conditions, see a suppression of their activity. In this specific case, methanogens are the most negatively affected by the salinity [13]. Their low capacity to acclimate to these conditions promotes the proliferation of other organisms of interest, such as acidogens, which are considered much more resilient under the same saline conditions, favouring VFA production and accumulation [14,15]. This allows the valorisation of highly saline wastewaters produced, for example, by the fish-canning industry, known for their high levels of NaCl and the challenging conversion to biogas [16]. It is also of great interest as it's an industry shifting towards a circular economy, making exploring the synergy between AD processes and saline wastewaters interesting [17].

According to recent studies, there are other parameters that can affect the production of VFA. Micro-aeration, which consists of the introduction of small quantities of air/oxygen, has been implemented to promote certain steps in AD processes, such as hydrolysis and acidogenesis, and therefore stimulating the production of VFA [18]. Hydrolysis is reported to be the rate-limiting step in AD of high solids organic substrates such as municipal solid wastes and lignocellulosic biomass. Nevertheless, the implementation of micro-aeration strategies has been described in the literaturesas helping to surpass this limitation by promoting the production of extracellular hydrolytic enzymes, such as amylases, proteases and cellulases, by more abundant and diverse hydrolytic bacterial communities, therefore enhancing the hydrolysis of carbohydrates, proteins, and other complex organic substrates [19–21]. Since hydrolysis is improved, higher concentrations of soluble substrate that can be further used by fermentative bacteria to produce VFAs will be available. It may also enhance the formation of specific VFA. Lim et al. [19] described a shift in fermentation production pattern where acetic acid was metabolized for the synthesis of butyric acid, under micro-aeration conditions. Overall, micro-aeration promotes the diversity of the microbial community, therefore enhancing the system's stability through syntrophic interactions between microbial communities [21].

In this work, two continuous bioreactors were used to assess the effect of micro-aeration during acidogenesis of high-salinity wastewaters. Leachate of FW from a canteen, wastewater from a biodiesel industry, and brine from the fish-canning industry were used as substrates. Physical-chemical parameters were used to evaluate both systems' performances. Also, quantitative image analysis (QIA) techniques were used to assess the characteristics of the sludge.

2. Materials and Methods

2.1. Inoculum and substrate

Reactors were inoculated with anaerobic granular sludge from a brewery wastewater treatment plant (Super Bock, Porto, Portugal) at a final concentration of 15 $g{\cdot}L^{-1}$ of volatile solids (VS). Before inoculation, methanogens were inactivated by boiling the sludge at 100 °C for 10 min [22].

As substrate, a mixture of FW leachate from the university canteen (University of Minho, Braga, Portugal), wastewater resulting from biodiesel production, and brine from a fish-canning industry (North of Portugal) were used. The characterization of each wastewater is presented in Table 1. The chemical oxygen demand (COD) of the mixture was approximately 40 $g{\cdot}L^{-1}$ (20 $g{\cdot}L^{-1}$ of FW and 20 $g{\cdot}L^{-1}$ of biodiesel WW) (Table 2). Brine was added to the mixture to provide a final salinity of 20 $g{\cdot}L^{-1}$. To obtain FW leachate, FW from the canteen was first blended, using a grinder and mixed with tap water, allowing their homogenization. Then, this FW was autoclaved at 121 °C, for 20 min, and in the end, it was centrifuged at 15,000 g for 15 min and stored in the frozen until used. The mixture (FW, biodiesel WW and brine) that was fed to the reactors was characterized over time and had a composition of: 1.84 ± 1.24 $g{\cdot}L^{-1}$ of COD of lactic acid; 0.22 ± 0.13 $g{\cdot}L^{-1}$ of COD of formic acid; 0.66 ± 0.56 $g{\cdot}L^{-1}$ of COD of acetic acid; 0.44 ± 0.20 $g{\cdot}L^{-1}$ of COD of propionic acid; 0.02 ± 0.02 $g{\cdot}L^{-1}$ of COD of n-butyric acid. The remaining acids were not detected.

2.2. Experimental Set-Up and operation mode

Two bioreactors were operated in parallel to test the effect of micro-aeration in the production of VFA from wastewaters with high salinity content. R1 (anoxic reactor) was operated under anoxic conditions and R2 (microaerophilic reactor) under microaerophilic conditions promoted by applying micro-aeration. Both reactors were fed from the same feeding tank, that was kept refrigerated at 4 °C, under agitation and opened to the air. Micro-aeration was applied by pumping air in the reactor (Fig. 1, R2). Both reactors were made of plexiglass material, had a total volume of 2.25 L and a working volume of 2.1 L, and consisted of Expanded Granular Sludge Bed (EGSB) reactors with external liquid recirculation as presented in Fig. 1. Sludge was also recirculated to the reactors once per day. The reactors were operated under mesophilic conditions (37 °C). The operation period was divided into five main periods, according to the conditions applied: operation mode (batch or continuous); (un)control of pH; hydraulic retention time (HRT); and micro-aeration flow. Table 2 shows the variable conditions applied at each period. Periods I and II were for adaptation and the pH was not controlled. In period III, the pH of the feeding was controlled and kept at 7 by a pH controller HI8711E (Hanna Instruments, Woonsocket, Rhode Island, EUA) with NaOH (1 mol L^{-1}). Sodium bicarbonate was also added in a final concentration of 5 g L^{-1}. In period IV the micro-aeration rate was increased 10 times, from 0.03 to 0.3 L of oxygen, per L of reactor and per day ($L_{O2}\ L_{reactor}^{-1}\ d^{-1}$). Period IV was divided into 3 sub-periods since the reactors' operation was interrupted for some weeks (due to the COVID-19 pandemics). During these interruptions the reactors were kept in batch at ~ 20° C. In period V the HRT was increased from 8 days to 10 days.

Samples for VFA, COD, pH and salinity analysis, were collected at the outlet with a periodicity of 3 times per week. Samples for oxidation–reduction potential (ORP), salinity and image analysis were collected in the sampling port, once per week.

2.3. Analytical methods

For sludge analysis by QIA and to measure the ORP, all samples were collected from the inside of the reactors. Samples for VFA, soluble COD (sCOD) and ammonium quantification were collected from the outlet flow of the reactors, centrifuged at 15000 rpm for 10 min, and filtered

Table 1
Total COD (tCOD), total solids (TS), and volatile solids (VS) content of each wastewater.

	FW leachate			Biodiesel WW			Brine		
tCOD/g/L	47.9	±	4.5	63.3	±	2.8	20.1	±	7.9
TS/g kg^{-1}	37.1	±	1.1	40.6	±	1.1	189.0	±	1.9
VS/g kg^{-1}	34.2	±	0.8	14.4	±	0.7	11.8	±	0.4

Table 2
Operating Conditions in R1 and R2: operation mode; aeration rate; HRT; Organic Loading Rate applied in COD to the reactors (OLR-CODin); total (tCOD-in) and soluble COD (sCOD-in) of the influent. n.a. – not applied.

Period	Time/d	pH	Mode	Aeration rate (L_{O2} $L^{-1}_{reactor}$ d^{-1})			HRT(d)			OLR-COD in (g/L d^{-1})			tCOD-in (g/L)			sCOD-in (g/L)		
				R1	R2		R1	R2		R1	R2		R1	R2		R1	R2	
I	0–23	uncontrolled	batch	n.a.	0.03 ± 0.02		n.a.	n.a.		n.a.	n.a.		n.a.	n.a.		n.a.	n.a.	
II	23–58	uncontrolled	cont.	n.a.	0.06 ± 0.02		8.5 ± 1.0	8.5 ± 0.3		4.3 ± 0.4	4.6 ± 1.2		35 ± 4	36 ± 5		33 ± 3	33 ± 3	
III	58–158	controlled pH_{in}	cont.	n.a.	0.03 ± 0.03		8.1 ± 0.9	7.5 ± 0.8		4.7 ± 0.5	4.6 ± 0.4		36 ± 2	35 ± 2		33 ± 2	33 ± 2	
IV.1	158–183	controlled pH_{in}	cont.	n.a.	0.27 ± 0.08		9.2 ± 1.6	8.3 ± 0.0		4.2 ± 0.5	4.4 ± 0.3		37 ± 2	36 ± 2		33 ± 2	32 ± 3	
IV.2	183–260	controlled pH_{in}	cont.	n.a.	0.30 ± 0.02		8.9 ± 0.9	8.2 ± 0.7		4.2 ± 0.4	4.3 ± 0.4		35 ± 1	36 ± 1		33 ± 1	34 ± 1	
IV.3	260–340	controlled pH_{in}	cont.	n.a.	0.29 ± 0.02		8.7 ± 0.8	8.7 ± 0.9		4.3 ± 0.3	4.3 ± 0.4		36 ± 2	36 ± 2		33 ± 1	33 ± 2	
V	340–500	controlled pH_{in}	cont.	n.a.	0.28 ± 0.05		10.6 ± 0.7	10.5 ± 0.7		3.6 ± 0.5	3.6 ± 0.3		37 ± 4	37 ± 3		32 ± 2	32 ± 2	

through 0.2 μm nylon syringe filter. VFA were analysed by high-performance liquid chromatography (HPLC) (Jasco, Tokyo, Japan), using a Rezex™ ROA-Organic Acid H+ (8 %) (30 x 4.6 mm) (Phenomenex, Torrance, California, EUA), at 60 °C and with UV detection at 210 nm. Sulfuric acid (5 mmol L^{-1}) was the mobile phase used at 0.6 mL min^{-1}. Total and soluble COD, and ammonium, were analysed using cuvette test kits (Hach-Lange GmbH, Düsseldorf, Germany) and a DR 2800 spectrophotometer (Hach-Lange GmbH). Solids (total and volatile) were determined according to the Standard Methods [23]. ORP was measured using a multiparameter analyzer C533 (Consort bvba, Turnhout, Belgium) and an ORP electrode D 223 (VWR, Radnor, PA). pH and salinity were measured with a multiparameter analyzer C3010 (Consort). Gas production was quantified with a Ritter MilliGas counter (Dr.-Ing. Ritter Apparatebau GmbH, Bochum, Germany). Nevertheless, the micro-aeration masked the possible gas production, and did not allow to follow the gas production over time (Figure S1).

2.4. Calculations

VFA and lactic acid results are expressed in this work in g/L of COD. The theoretical COD equivalence for lactic, formic, acetic, propionic, butyric, valeric, and hexanoic acids were 1.07, 0.35, 1.07, 1.51, 1.82, 2.04, and 2.21 g of COD g^{-1} of acid, respectively, and were calculated according to [24].

The ratio between VFA+lactic acid (in COD) and the sCOD measured, was calculated according to Equation (1):

$$VFA/sCOD(\%, w/w) = \frac{COD_{VFA} + COD_{lactic\ acid}}{sCOD} \times 100 \quad (1)$$

The degree of acidification (DOA) was defined as the ratio between the total VFA+lactic acid (in COD) in the reactor and the tCOD fed to the reactors, according to Equation (2):

$$DOA(\%, w/w) = \frac{COD_{VFA} + COD_{lactic\ acid}}{tCOD} \times 100 \quad (2)$$

2.5. Image acquisition, processing, and analysis

For sludge characterization bright-field microscopy was used to acquire images from both reactors along operation. A recalibrated micropipette, with a sectioned tip was used in order to flow larger aggregates. For each sample, 10 μL of biomass was placed on the slides, in triplicates, and covered with a 20 mm x 20 mm cover slip [25]. An Olympus BX51 microscope (Olympus, Tokyo, Japan) coupled to an Olympus DP71 camera (Olympus, Shinjuku, Japan) was used for image visualization and acquisition. The completed analysis resulted in a total of 150 images (3 × 50 image per slide), acquired at 100 × total magnification with cellSens software (Olympus, Shinjuku, Japan) at 1360 × 1024 pixels, in a 8-bit format. For image processing, Matlab R2023a (The Mathworks, Natich, USA) was used, being divided in: pre-treatment, segmentation and debris elimination, and QIA parameters determination. Detailed description of the image processing steps can be found elsewhere [26]. From the resulting binary images, aggregates and filaments were characterized. Aggregates were divided into 2 size classes according to their equivalent diameter (Deq): small (<25 μm) and intermediate (25–250 μm). QIA parameters obtained from the processed images can be found elsewhere [27], and were divided into 4 main descriptor groups: (i) free filamentous bacteria content, (ii) aggregates size, (iii) aggregates content, and (iv) aggregates morphology (Supplementary information, Table S1).

2.6. Principal component analysis (PCA)

PCA enables the identification of the most important information about the new spaces created by principal components (PC) describing a linear combination of the original variables. For this, a total of 68

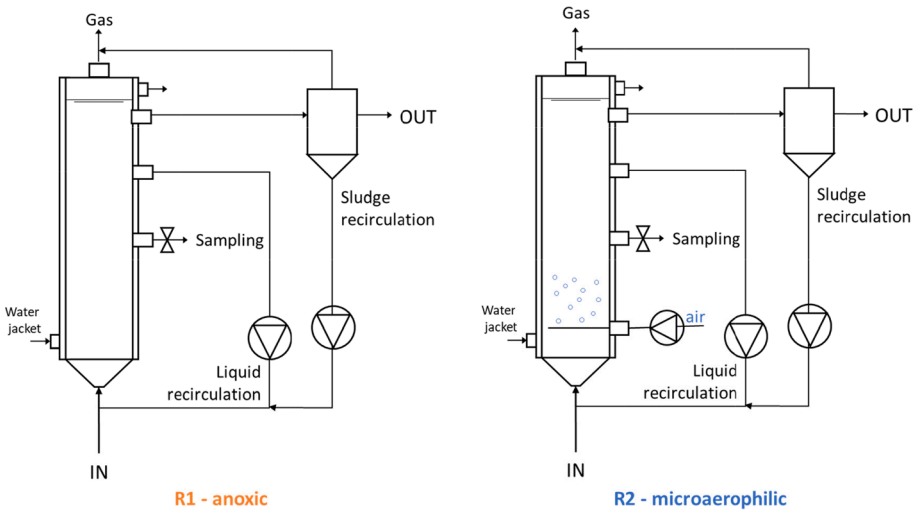

Fig. 1. Schematic diagram of the experimental setup.

observations and 35 variables were used to compose the dataset matrix. The goal of the employed PCA was to establish key interrelationships between the parameters that compose the dataset matrix and evaluate the differentiation between R1 (anoxic) and R2 (microaerophilic) bioreactors. The PCA was performed with Matlab R2023a software (The MathWorks, Inc. Natick, USA).

3. Results

Micro-aeration was tested as a strategy to improve VFA production and potentially induce a shift in the VFA profile. Two bioreactors, a control reactor operated under anoxic condition (R1), and a micro-aerated reactor (R2), were operated and their performance regarding VFA production was compared. Reactors' operation was divided into 5 main periods, described in the previous section.

Fig. 2 shows the variation of pH and ORP over time in both reactors. In periods I-III, when the aeration rate was lower and around 0.03 L_{O2} $L^{-1}_{reactor}$ d^{-1} (Table 2), the ORP varied similarly in both reactors. In periods IV and V, in certain phases, such as in the time intervals of 183–250 days (period IV.2) and 400–450 days (period V), the ORP reached lower values (with approximately 100 mV of difference) in R2 (micro-aerated bioreactor). In the overall ORP values were always negative. Regarding the pH, until day 50 (periods I-II), since no control was applied, the pH decreased to values around 4, in both reactors and feeding. After

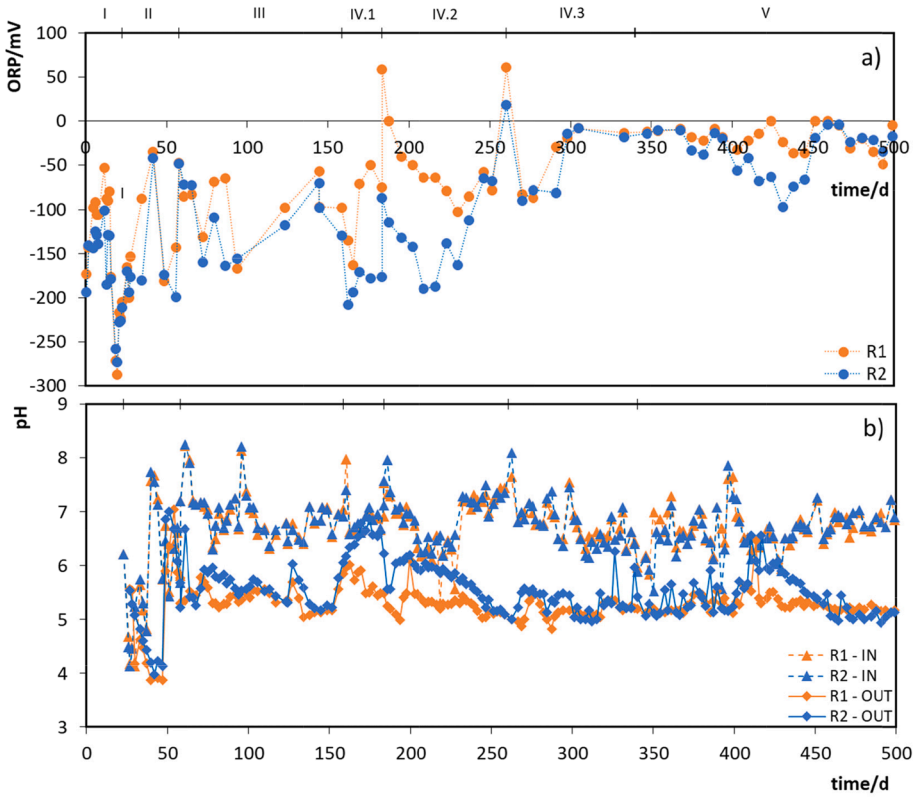

Fig. 2. ORP (a) and pH (b) profiles in reactors R1 and R2. ORP values are of samples collected from the inside of the reactors. pH values were measured in the inlet (IN) and outlet (OUT) of the reactors.

applying pH control in the feeding, pH values varied around neutrality (between 6 and 8), and slightly acidic (between 5 and 6) in the reactors. In periods IV (particularly in IV.1 and IV.2) and V (400–450 days), the pH was slightly higher in R2 than in R1, when compared to the other periods, in which the pH in both reactors were very similar.

The soluble COD in the fermented broth obtained from both reactors was constant over time and similar in both reactors (Table 3). Regarding the ratio VFA/sCOD and the DOA, in general no differences between the reactors were observed.

In period I, lactic acid was the predominant acid reaching, on average, 35 % of the total VFA (Table 4) production. Its maximum concentration was of 7 g L^{-1} of COD in both reactors, as it is possible to observe in Fig. 3. In period II, in addition to lactic acid, n-butyric became dominant in both R1 and R2. In periods III, IV and V, iso- and n-butyric acids were the principal VFA produced in both reactors (Fig. 3), and their sum varied from 40 % to 60 % of total VFA. Over time, the n-valeric acid became more representative in both reactors, reaching around 20 % of total VFA in period V. The main difference observed between the R1 and the R2 occurred in period IV.2, when n-hexanoic concentration became 3 times higher in R2 (25 % ± 7 %) than in R1 (7 % ± 3 %), as it is possible to confirm in Table 4 and Fig. 3.

Ammonium concentration, probably resulting from proteins degradation, was quantified and its profile is presented in Fig. 4. In period III ammonium concentration was higher in R2 in comparison with R1, reaching a maximum of 568 mg L^{-1}. Higher values around 600 mg L^{-1} were observed in both reactors solely during IV.1. Ammonium nitrogen has been studied as an indicator of protein degradation in anaerobic digestion [28]. A previous study revealed that a higher ammonium concentration most likely indicates that there was more protein degradation compared to the low ammonia concentration [29]. From period IV.2 onwards, ammonium concentrations decreased and became very similar in both R1 and R2.

PCA was employed to handle the substantial volume of data generated by QIA. Each principal component (PC) provides scores that depict the relationship between sample points, as well as loadings that indicate the influence of variables on the corresponding PC (Fig. 5). The first and second PCs derived from PCA accounted for 57.99 % of the dataset's variance. In Fig. 5a, two prominent clusters are evident, representing the morphological variations in the sludge throughout the bioreactor's operation. The left cluster exhibits negative scores in PC1 and a wide range of scores in PC2, predominantly comprising observations from the R1 (anoxic) bioreactor. On the other hand, the right cluster encompasses the remaining sludge observations from the R2 (microaerophilic) bioreactor. Therefore, PC1 effectively discriminates between the two reactors, facilitating their clear differentiation.

The R1 cluster demonstrates a positive association with changes in the size (Per_i, L_i, W_i, Deq_i, Area_i) and content (Area/vol_i, %Area_i) of intermediate aggregates (Fig. 5a,b, Figure S2a). Conversely, the parameters that predominantly contribute to the positive influence on the R2 cluster are mainly associated with the morphology of intermediate aggregates (Conv_i, Sol_i, Round_i) and the content of small aggregates (%Area_s) (Fig. 5a,b, Figure S2a). When examining the sludge observations from R1 and R2, it is evident that they shift along the PC2 axis. This shift is primarily driven by both the size parameters of small aggregates (L_s, Per_s, Area_s, Deq_s) (observations located at the top) and the size parameters of intermediate aggregates (Area_i, Deq_i, W_i, L_i) (observations located at the bottom) (Fig. 5a,b, Figure S2b).

4. Discussion

It has been described that increasing salt concentration (>8 g/L), may promote methanogenesis inhibition and potentially inhibit VFA production during acidogenesis [20,30]. Nevertheless, this work does not corroborate this statement. Two bioreactors were operated over 500 days, fed with leachate from food waste of a canteen (which may present some fluctuation in its composition), wastewater resulting from biodiesel production, and brine, with a final salinity content around 20 g·L^{-1}. Over time the soluble COD in both reactors remained constant (approximately 30 g/L) and similar (Table 3). In the first periods (I and II) pH was not controlled, which resulted in lactic acid accumulation, lower DOA (between 28 % and 53 %, on average), and absence or lower concentrations of longer fatty acids, such as valeric and hexanoic acids (Tables 3, 4 and Fig. 3). Then, under controlled pH in periods III, IV and V the ratio VFA/sCOD varied slightly between 63 % and 80 %, on average. Those results show the absence of acidogenic inhibition due to 20 g L^{-1} of salinity. Acidogenic bacteria are known as being less sensitive to salinity than methanogens, which explains the usually fatty acid accumulation and methanogenesis suppression at high salt concentrations [15]. Moreover, high salinity also has been described as promoting shifts in the microbial community, towards a community more resilient and resistant to osmotic stress [31]. Previous works showed high VFA yields under 20 g L^{-1} of salinity [15,24,32], being 30 g L^{-1} already described as inhibiting acidogenesis of food waste [12,32]. In the present work, the best results obtained in the presence of 20 g L^{-1} of salinity were in period IV.2 (in both reactors), where a maximum average of 80 % of sCOD as VFA (~70 % of DOA) was reached. Those values were slightly higher than the ones obtained by other authors using FW leachate and 20 g L^{-1} of salinity, who obtained 60 % of DOA [15]. These authors reported similar percentages of VFAs: 33 % acetate, 16 % propionate, 40 % butyrate, and 11 % valerate. In our study, we observed acetate (<22 %), valerate (13–20 %), and occasional hexanoate (Table 4). The differences in acid production are relatively small and comparable to the literature. This consistency of results over reactors' operation, when compared with other works, shows the robustness of this co-digestion process.

One of the strategies suggested to boost VFA production, or even mitigate acidogenesis inhibition through salinity is the implementation of micro-aeration [18]. Since air-nanobubbles are negatively charged, they can combine with cations (Na^{+}), decreasing the osmotic pressure on microbial cells caused by salinity [20]. The work of Hou et al. [20] showed that with increasing salt concentrations, higher total VFA productions were achieved when micro-aeration through air-nanobubbles was applied to the reactors, not only due to the effect of air-nanobubbles on the salt cations, but also due to the enhanced the activities of the electron transport system and extracellular hydrolases. Also, over the last decade, several works have shown the

Table 3
Soluble COD (sCOD), ratio VFA to sCOD (VFA/sCOD) and DOA in the reactors' outlet.

Period	sCOD-out (g/L)						VFA/sCOD(%)						DOA(%)					
	R1			R2			R1			R2			R1			R2		
I	32	±	1	32	±	1	37	±	22	28	±	9	37	±	22	28	±	9
II	31	±	1	30	±	2	59	±	7	47	±	7	53	±	9	39	±	6
III	31	±	1	31	±	2	65	±	8	66	±	10	57	±	8	57	±	8
IV.1	31	±	1	29	±	2	69	±	13	60	±	7	58	±	11	48	±	5
IV.2	31	±	1	30	±	1	80	±	22	77	±	19	71	±	20	64	±	14
IV.3	31	±	1	29	±	2	60	±	6	63	±	8	52	±	6	50	±	6
V	30	±	1	27	±	2	70	±	5	73	±	10	57	±	9	54	±	7

Table 4
Average of VFA composition in each period and reactor.

Period	Lactic			Formic			Acetic			Propionic			*iso*-butyric		
	R1		R2	R1		R2	R1		R2	R1		R2	R1		R2
I	35 %	± 26 %	35 %	± 25 %	± 0 %	0 %	± 16 %	± 8 %	23 %	± 8 %	6 %	± 2 %	14 %	± 8 %	1 %	± 1 %	0 %	± 0 %
II	21 %	± 25 %	18 %	± 22 %	± 0 %	1 %	± 8 %	± 4 %	9 %	± 4 %	8 %	± 7 %	18 %	± 7 %	3 %	± 5 %	1 %	± 1 %
III	1 %	± 2 %	1 %	± 2 %	± 0 %	0 %	± 13 %	± 3 %	15 %	± 5 %	8 %	± 4 %	11 %	± 9 %	28 %	± 7 %	21 %	± 9 %
IV.1	0 %	± 0 %	0 %	± 0 %	± 0 %	0 %	± 19 %	± 2 %	22 %	± 1 %	8 %	± 5 %	13 %	± 3 %	26 %	± 5 %	14 %	± 2 %
IV.2	1 %	± 4 %	0 %	± 1 %	± 0 %	0 %	± 14 %	± 3 %	13 %	± 3 %	11 %	± 6 %	6 %	± 5 %	21 %	± 7 %	20 %	± 7 %
IV.3	2 %	± 4 %	1 %	± 1 %	± 0 %	0 %	± 15 %	± 2 %	15 %	± 3 %	11 %	± 5 %	10 %	± 4 %	23 %	± 5 %	28 %	± 5 %
V	1 %	± 2 %	1 %	± 2 %	± 0 %	0 %	± 13 %	± 2 %	14 %	± 3 %	8 %	± 4 %	8 %	± 2 %	25 %	± 4 %	28 %	± 7 %

Period	*n*-butyric			*iso*-valeric			*n*-valeric			*iso*-hexanoic			*n*-hexanoic		
	R1		R2	R1		R2	R1		R2	R1		R2	R1		R2
I	10 %	± 10 %	13 %	± 18 %	± 10 %	13 %	± 7 %	± 1 %	2 %	± 2 %	3 %	± 13 %	0 %	± 0 %	1 %	± 4 %	0 %	± 0 %
II	30 %	± 12 %	48 %	± 14 %	± 1 %	2 %	± 1 %	± 3 %	1 %	± 1 %	0 %	± 0 %	0 %	± 0 %	5 %	± 4 %	1 %	± 1 %
III	26 %	± 8 %	26 %	± 7 %	± 1 %	2 %	± 2 %	± 13 %	13 %	± 4 %	0 %	± 0 %	0 %	± 1 %	9 %	± 4 %	11 %	± 4 %
IV.1	23 %	± 3 %	30 %	± 3 %	± 2 %	2 %	± 3 %	± 15 %	9 %	± 1 %	1 %	± 1 %	1 %	± 1 %	7 %	± 4 %	8 %	± 4 %
IV.2	27 %	± 5 %	20 %	± 4 %	± 1 %	1 %	± 1 %	± 17 %	14 %	± 4 %	0 %	± 1 %	1 %	± 2 %	7 %	± 3 %	25 %	± 7 %
IV.3	23 %	± 3 %	21 %	± 3 %	± 2 %	2 %	± 1 %	± 18 %	18 %	± 2 %	1 %	± 1 %	1 %	± 1 %	4 %	± 2 %	6 %	± 3 %
V	27 %	± 6 %	24 %	± 6 %	± 1 %	1 %	± 1 %	± 22 %	20 %	± 3 %	0 %	± 1 %	0 %	± 0 %	4 %	± 2 %	4 %	± 3 %

implementation of micro-aeration as an advantageous strategy to improve hydrolysis and acidogenesis in AD systems [21,33,34]. To study micro-aeration process, due to the fast consumption of oxygen and the low detection limit of oxygen-dissolved (DO) probes (−50 mV corresponds to the detection limit of DO probe at 0.1 mg/L), variations in oxygen concentration in the liquid phase are usually evaluated by the ORP, which varies linearly with the logarithm of oxygen concentration [21]. By implementing micro-aeration during acidogenic fermentation, ORP levels between −100 mV and −200 mV were specified for VFA production in previous works [35]. Additionally, ORP in the anaerobic region between −200 mV and −300 mV was not appropriate for VFA synthesis [35]. In our work, the ORP in the micro-aerated bioreactor (R2) was on average lower than in the anaerobic one (R1), particularly in periods IV.2 and V (Fig. 2a), indicating that the O_2 concentration in R2 was lower than in R1. This seems to suggest that micro-aeration in R2 potentiated the activity or growth of aerobic or facultative microorganisms that were able to consume the O_2 available, reducing the ORP to more negative values (−200 mV in period IV.2 and −100 mV in period V, Fig. 2a).

After exposure to micro-aeration, an increase of bacterial activity of hydrolytic and fermentative bacterial communities has been described [21]. For example, Lim et al. [19] reported an increase in abundance of the Firmicutes phylum (especially in Clostridia and Bacilli class), which resulted in a 3-fold increase in acetated and butyrate concentrations. This might be the result of the direct use of oxygen by the fermentative bacteria that produces VFA, but also the indirect effect of promoting hydrolysis. Micro-aeration thus provides a controlled environment where the benefits of limited oxygen exposure can be employed without disrupting the anaerobic processes essential for VFA production. Therefore, facultative and obligatory anaerobic bacteria may cohabit in a special habitat created by micro-aeration [36]. During this time, facultative microbes could consume any traces of O_2 and maintain anaerobic conditions for obligate anaerobic microorganisms to thrive [37]. Under ORP conditions higher than − 200 mV, as it has been observed for the majority of time in both reactors, in the absence of nitrate (and therefore nitrification), usually facultative fermentation occurs [37].

It has been previously suggested that low O_2 levels may support the production of medium-chain fatty acids, such as hexanoic acid, in acidogenic bioreactors, by supporting lactate (electron donor in chain elongation) production pathways over other metabolic routes that are more oxygen-sensitive [38,39]. Notably, the enzymes governing the chain-elongation process exhibit reduced sensitivity to low oxygen levels, enabling efficient operation even in micro-aerobic conditions [18]. This may be the case of what happened during period IV.2, in which hexanoate concentration was on average 3.5x higher in R2 than in R1 (Table 4). Also, Liu et al [40] have observed more hexanoic production from cow manure, under micro-aeration conditions (though air-nanobubbles). These authors related this behaviour with the fact that air-nanobubbles may enhance the electron transfer capacity of the AD system, accelerating the redox reaction of the chain-elongation process; and that micro-aeration facilitated the decomposition of recalcitrant organic matter, leading to an improved substrate utilization rate.

Particulate matter undergoes hydrolysis when extracellular enzymes produced by hydrolytic bacteria break down and solubilize it. Since more hydrolytic enzymes are produced under aerobic than anaerobic conditions, hydrolysis efficiency is known to be higher under the aerobic ones [34]. Therefore, it is expected that the intensity of micro-aeration may conditionate the hydrolysis efficiency and also the degree of acidification [34]. In the study of Lim and Wang (2013), a micro-aeration rate of 0.0375 L_{O2} $L_{reactor}^{-1}$ d^{-1}, increased the solubilization of organic matter during the co-digestion of brown water and FW, without the oxygen-related inhibition of acidogenesis [34]. In the present work, similar micro-aeration conditions were applied in Periods I to III (Table 2). However, no differences between both reactors were observed regarding the sCOD profile (Table 3), nor when the micro-aeration rate

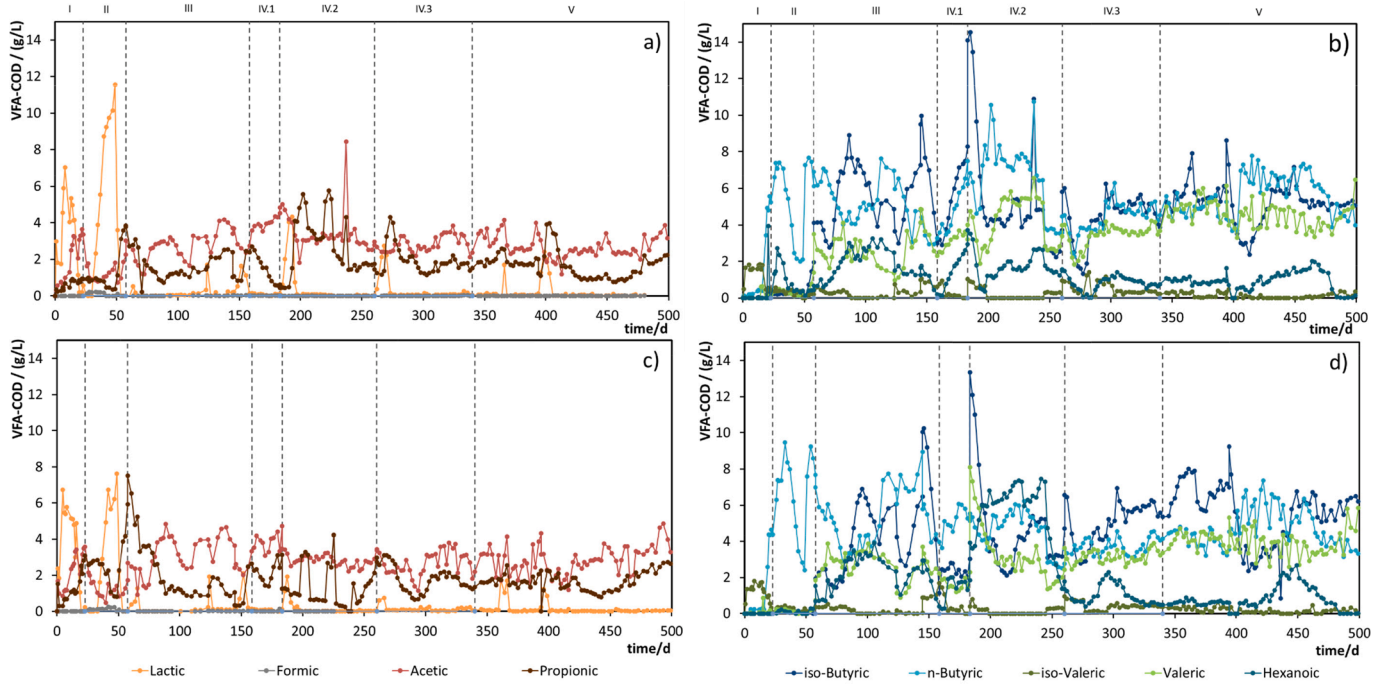

Fig. 3. VFA and lactic acid profiles (in COD) in reactors R1 (a, b) and R2 (c, d), over time.

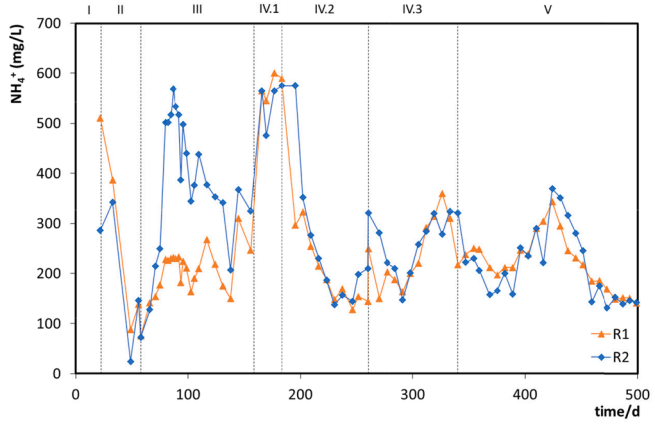

Fig. 4. Ammonium concentration in reactors R1 and R2 over time.

was increased 10x in R2 (Periods IV and V) (Table 3).

Previous studies have extensively explored the application of PCA in AD. On one hand, studies have demonstrated that PCA plays a crucial role in improving decision-making, reducing costs, and enhancing operational efficiency in AD processes [41]. On the other hand, the integration of PCA and QIA parameters has shown significant potential in evaluating the toxic shock load effects on anaerobic granular sludge, favouring the optimization and management of AD processes, as well as ensuring their sustainability and efficiency [42]. The current PCA analysis has a specific objective, which is to assess the QIA aggregates parameters derived from the sludge samples obtained from the R1 (anoxic) and R2 (microaerophilic) bioreactors. The purpose of this analysis is to examine and understand the variations and patterns in the QIA parameters within these two types of bioreactors. During the operation of each bioreactor, fluctuations in the aggregates size were consistently observed and evidenced by the variations in the PCA scores plot (Fig. 5a). This plot illustrates the distribution of the samples based on their aggregate size-related variables as demonstrated in the PCA loading plot (Fig. 5b). The top part of the PCA scores plot represents the

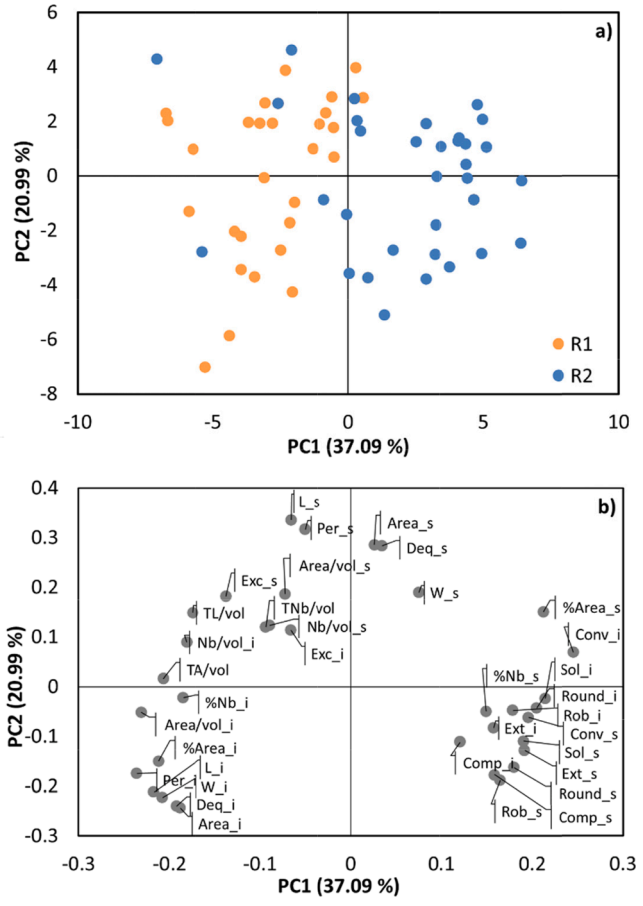

Fig. 5. (a) PCA scores plot of the QIA dataset for PC1 vs PC2 of R1 and R2. (b) PCA loadings plot for PC1 vs PC2.

observations impacted by the size of small aggregates variables, while the bottom part represents observations impacted by the variables related to the size of intermediate aggregates (Figure S2b).

Previous research has established that reactor configurations, hydrodynamic conditions, including shear forces, mixing intensity, and flow regimes [43,44], as well as aeration [45], play vital roles in achieving optimal treatment performance and solids separation in aerobic processes. In the present case, the results clearly demonstrate a noticeable distinction between the observations from R1 and R2 in the PCA scores plot, highlighting the significant impact of micro-aeration on the morphology of intermediate aggregates. The variations in Conv_i, Sol_i, and Round_i morphological descriptors further accentuate this distinction (Fig. 5, Figure S2a).

These findings emphasize the strong relationship between micro-aeration and the dynamic nature of aggregates morphology and size during VFA production.

5. Conclusions

Waste valorization is a fundamental practice to adopt in current and future societies. In the present study, the efficiency of AD in the production of VFA, using FW leachate from a canteen, wastewater from biodiesel industry and brine from fish-canning industry were used, solidifying the robustness and efficiency of the process. It was observed that salinity (20 g L^{-1}) does not inhibit acidogenesis, contrary to what is referred in some studies. This conclusion is supported by consistent values of COD and VFA/sCOD ratio observed in both reactors, R1 and R2. The percentages of formed VFA are in accordance with the literature, despite the lower values of acetate, the higher values of valerate, and the higher DOA percentages (70 %) obtained in our study.

Regarding micro-aeration, some differences can be pointed out between reactors. R2 demonstrated lower ORP values in periods IV.2 and V, due to the growth of aerobic or facultative microorganisms, which is a consequence of O_2 input. Also, a higher formation of hexanoic acid was observed in R2 in period IV.2, which can be a consequence of the lower values of O_2 concentration (accessed by ORP) in R2. PCA analysis and QIA aggregates parameters demonstrated considerable differences between R1 and R2, particularly in terms of aggregates size and morphology when subjected to micro-aeration. Overall, the results demonstrated the stability and consistency of the process, despite the high salinity, with micro-aeration positively affecting some physico-chemical parameters and sludge.

CRediT authorship contribution statement

M. Salomé Duarte: Writing – review & editing, Writing – original draft, Validation, Methodology, Investigation, Formal analysis, Data curation, Conceptualization. **Ricardo J.C. Fernandes:** Writing – original draft, Methodology, Investigation. **João Sousa:** Investigation. **Carla Pereira:** Methodology, Investigation. **Daniela P. Mesquita:** Writing – review & editing, Supervision, Project administration, Methodology, Investigation, Data curation, Conceptualization. **M. Madalena Alves:** Writing – review & editing, Validation, Supervision, Methodology, Funding acquisition, Formal analysis, Conceptualization.

Declaration of competing interest

The authors declare that they have no known competing financial interests or personal relationships that could have appeared to influence the work reported in this paper.

Data availability

Data will be made available on request.

Acknowledgments

This study was supported by the Portuguese Foundation for Science and Technology (FCT) under the scope of the strategic funding of the UIDB/04469/2020 unit. Research of R. Fernandes, C. Pereira and J. Sousa was supported by the SALTIPHA project (PTDC/BTA-BTA/30902/2017), under the funding program 02/SAICT/2017 - Projetos de Investigação Científica e Desenvolvimento Tecnológico (IC&DT) with reference NORTE-01-0145-FEDER-030902. M. Salomé Duarte acknowledges FCT for the Junior Research contract obtained under the scope of the Scientific Stimulus Employment 2022 with the reference 2022.06569.CEECIND/CP1718/CT0004 (DOI: 10.54499/2022.06569.CEECIND/CP1718/CT0004). Daniela P. Mesquita acknowledges FCT funding under CEEC INST 2ed (CEECINST/00018/2021/CP2806/CT0004; DOI: 10.54499/CEECINST/00018/2021/CP2806/CT0004).

Appendix A. Supplementary data

Supplementary data to this article can be found online at https://doi.org/10.1016/j.fuel.2024.132566.

References

[1] Magnusson T, Zanatta H, Larsson M, Kanda W, Hjelm O. Circular economy, varieties of capitalism and technology diffusion: Anaerobic digestion in Sweden and Paraná. J Clean Prod 2022;335:130300. https://doi.org/10.1016/j.jclepro.2021.130300.
[2] Lee JTE, Ok YS, Song S, Dissanayake PD, Tian H, Tio ZK, et al. Biochar utilisation in the anaerobic digestion of food waste for the creation of a circular economy via biogas upgrading and digestate treatment. Bioresour Technol 2021;333:125190. https://doi.org/10.1016/j.biortech.2021.125190.
[3] Pandey P, Lejeune M, Biswas S, Morash D, Weimer B, Young G. A new method for converting foodwaste into pathogen free soil amendment for enhancing agricultural sustainability. J Clean Prod 2016;112:205–13. https://doi.org/10.1016/j.jclepro.2015.09.045.
[4] Gomes K, Guenther E, Morris J, Miggelbrink J, Caucci S. Resource nexus oriented decision making along the textile value chain: The case of wastewater management. Curr Res Environ Sustain 2022;4:100153. https://doi.org/10.1016/j.crsust.2022.100153.
[5] Xu F, Okopi SI, Jiang Y, Chen Z, Meng L, Li Y, et al. Multi-criteria assessment of food waste and waste paper anaerobic co-digestion: Effects of inoculation ratio, total solids content, and feedstock composition. Renew Energy 2022;194:40–50. https://doi.org/10.1016/j.renene.2022.05.078.
[6] Feng S, Ngo HH, Guo W, Chang SW, Nguyen DD, Liu Y, et al. Volatile fatty acids production from waste streams by anaerobic digestion: A critical review of the roles and application of enzymes. Bioresour Technol 2022;359:127420. https://doi.org/10.1016/j.biortech.2022.127420.
[7] Pandey AK, Pilli S, Bhunia P, Tyagi RD, Surampalli RY, Zhang TC, et al. Dark fermentation: Production and utilization of volatile fatty acid from different wastes- A review. Chemosphere 2022;288:132444. https://doi.org/10.1016/j.chemosphere.2021.132444.
[8] Castro-Fernandez A, Rodríguez-Hernández L, Castro-Barros CM, Lema JM, Taboada-Santos A. Scale-up and economic assessment of volatile fatty acids production from food waste. Biomass Bioenergy 2024;182. https://doi.org/10.1016/j.biombioe.2024.107112.
[9] Bose RS, Zakaria BS, Dhar BR, Tiwari MK. Effect of salinity and surfactant on volatile fatty acids production from kitchen wastewater fermentation. Bioresour Technol Reports 2022;18:101017. https://doi.org/10.1016/j.biteb.2022.101017.
[10] Wang L, Hao J, Wang C, Li Y, Yang Q. Carbohydrate-to-protein ratio regulates hydrolysis and acidogenesis processes during volatile fatty acids production. Bioresour Technol 2022;355:127266. https://doi.org/10.1016/j.biortech.2022.127266.
[11] Jiang J, Zhang Y, Li K, Wang Q, Gong C, Li M. Volatile fatty acids production from food waste: Effects of pH, temperature, and organic loading rate. Bioresour Technol 2013;143:525–30. https://doi.org/10.1016/j.biortech.2013.06.025.
[12] He X, Yin J, Liu J, Chen T, Shen D. Characteristics of acidogenic fermentation for volatile fatty acid production from food waste at high concentrations of NaCl. Bioresour Technol 2019;271:244–50. https://doi.org/10.1016/j.biortech.2018.09.116.
[13] Hendriks ATWM, van Lier JB, de Kreuk MK. Growth media in anaerobic fermentative processes: The underestimated potential of thermophilic fermentation and anaerobic digestion. Biotechnol Adv 2018;36:1–13. https://doi.org/10.1016/j.biotechadv.2017.08.004.
[14] Fra-Vázquez A, Pedrouso A, Val del Rio A, Mosquera-Corral A. Volatile fatty acid production from saline cooked mussel processing wastewater at low pH. Sci Total Environ 2020;732:139337. https://doi.org/10.1016/j.scitotenv.2020.139337.
[15] Sarkar O, Kiran Katari J, Chatterjee S, Venkata MS. Salinity induced acidogenic fermentation of food waste regulates biohydrogen production and volatile fatty acids profile. Fuel 2020;276:117794. https://doi.org/10.1016/j.fuel.2020.117794.

[16] Picos-Benítez AR, Peralta-Hernández JM, López-Hincapié JD, Rodríguez-García A. Biogas production from saline wastewater of the evisceration process of the fish processing industry. J Water Process Eng 2019;32:100933. https://doi.org/10.1016/j.jwpe.2019.100933.
[17] Fernández-González R, Teixeira Pereira ZG, Ricoy-Casas RM. Governance of the circular economy in the canned fish industry: A case study from Spain. Environ Technol Innov 2024;(34). https://doi.org/10.1016/j.eti.2024.103618.
[18] Chen Q, Wu W, Qi D, Ding Y, Zhao Z. Review on microaeration-based anaerobic digestion: State of the art, challenges, and prospectives. Sci Total Environ 2020;710:136388. https://doi.org/10.1016/j.scitotenv.2019.136388.
[19] Lim JW, Chiam JA, Wang JY. Microbial community structure reveals how microaeration improves fermentation during anaerobic co-digestion of brown water and food waste. Bioresour Technol 2014;171:132–8. https://doi.org/10.1016/j.biortech.2014.08.050.
[20] Hou T, Zhao J, Lei Z, Shimizu K, Zhang Z. Addition of air-nanobubble water to mitigate the inhibition of high salinity on co-production of hydrogen and methane from two-stage anaerobic digestion of food waste. J Clean Prod 2021;314:127942. https://doi.org/10.1016/j.jclepro.2021.127942.
[21] Nguyen D, Khanal SK. A little breath of fresh air into an anaerobic system: How microaeration facilitates anaerobic digestion process. Biotechnol Adv 2018;36:1971–83. https://doi.org/10.1016/j.biotechadv.2018.08.007.
[22] Abreu AA, Alves JI, Pereira MA, Sousa DZ, Alves MM. Strategies to suppress hydrogen-consuming microorganisms affect macro and micro scale structure and microbiology of granular sludge. Biotechnol Bioeng 2011;108:1766–75. https://doi.org/10.1002/bit.23145.
[23] APHA, AWWA, WPCF. Standard Methods for the Examination of Water and Wastewater. Washington D.C., USA: American Public Health Association; 1999.
[24] Duarte MS, Oliveira JV, Pereira C, Carvalho M, Mesquita DP, Alves MM. Volatile fatty acids (VFA) production from wastewaters with high salinity—influence of pH. Salinity and Reactor Configuration Fermentation 2021;7:303. https://doi.org/10.3390/fermentation7040303.
[25] Mesquita DPP, Amaral ALL, Ferreira ECC. Identifying different types of bulking in an activated sludge system through quantitative image analysis. Chemosphere 2011;85:643–52. https://doi.org/10.1016/j.chemosphere.2011.07.012.
[26] Mesquita DP, Amaral AL, Ferreira EC. Estimation of effluent quality parameters from an activated sludge system using quantitative image analysis. Chem Eng J 2016;285:349–57. https://doi.org/10.1016/j.cej.2015.09.110.
[27] Costa JG, Paulo AMS, Amorim CL, Amaral AL, Castro PML, Ferreira EC, et al. Quantitative image analysis as a robust tool to assess effluent quality from an aerobic granular sludge system treating industrial wastewater. Chemosphere 2022;291. https://doi.org/10.1016/j.chemosphere.2021.132773.
[28] Yang G, Zhang P, Zhang G, Wang Y, Yang A. Degradation properties of protein and carbohydrate during sludge anaerobic digestion. Bioresour Technol 2015;192:126–30. https://doi.org/10.1016/j.biortech.2015.05.076.
[29] Lukitawesa PRJ, Millati R, Sárvári-Horváth I, Taherzadeh MJ. Factors influencing volatile fatty acids production from food wastes via anaerobic digestion. Bioengineered 2020;11:39–52. https://doi.org/10.1080/21655979.2019.1703544.
[30] Zhao J, Zhang C, Wang D, Li X, An H, Xie T, et al. Revealing the underlying mechanisms of how sodium chloride affects short-chain fatty acid production from the cofermentation of waste activated sludge and food waste. ACS Sustain Chem Eng 2016;4:4675–84. https://doi.org/10.1021/acssuschemeng.6b00816.
[31] Huang J, Pan Y, Liu L, Liang J, Wu L, Zhu H, et al. High salinity slowed organic acid production from acidogenic fermentation of kitchen wastewater by shaping functional bacterial community. J Environ Manage 2022;310:114765. https://doi.org/10.1016/j.jenvman.2022.114765.
[32] Li X, Sadiq S, Zhang W, Chen Y, Xu X, Abbas A, et al. Salinity enhances high optically active L-lactate production from co-fermentation of food waste and waste activated sludge: Unveiling the response of microbial community shift and functional profiling. Bioresour Technol 2021;319:124124. https://doi.org/10.1016/j.biortech.2020.124124.
[33] Xu S, Selvam A, Wong JWC. Optimization of micro-aeration intensity in acidogenic reactor of a two-phase anaerobic digester treating food waste. Waste Manag 2014;34:363–9. https://doi.org/10.1016/j.wasman.2013.10.038.
[34] Lim JW, Wang JY. Enhanced hydrolysis and methane yield by applying microaeration pretreatment to the anaerobic co-digestion of brown water and food waste. Waste Manag 2013;33:813–9. https://doi.org/10.1016/j.wasman.2012.11.013.
[35] Yin J, Yu X, Zhang Y, Shen D, Wang M, Long Y, et al. Enhancement of acidogenic fermentation for volatile fatty acid production from food waste: Effect of redox potential and inoculum. Bioresour Technol 2016;216:996–1003. https://doi.org/10.1016/j.biortech.2016.06.053.
[36] Cao Q, Zhang W, Lian T, Wang S, Yin F, Zhou T, et al. Roles of micro-aeration on enhancing volatile fatty acids and lactic acid production from agricultural wastes. Bioresour Technol 2022;347:126656. https://doi.org/10.1016/j.biortech.2021.126656.
[37] Fu S, Lian S, Angelidaki I, Guo R. Micro-aeration: an attractive strategy to facilitate anaerobic digestion. Trends Biotechnol 2022:1–13. https://doi.org/10.1016/j.tibtech.2022.09.008.
[38] Magdalena JA, Angenent LT, Usack JG. The measurement, application, and effect of oxygen in microbial fermentations: Focusing on methane and carboxylate production. Fermentation 2022;8. https://doi.org/10.3390/fermentation8040138.
[39] Lambrecht J, Cichocki N, Schattenberg F, Kleinsteuber S, Harms H, Müller S, et al. Key sub-community dynamics of medium-chain carboxylate production. Microb Cell Fact 2019;18:1–17. https://doi.org/10.1186/s12934-019-1143-8.
[40] Liu Y, Ye X, Chen K, Wu X, Jiao L, Zhang H, et al. Effect of nanobubble water on medium chain carboxylic acids production in anaerobic digestion of cow manure. Waste Manag 2024;184:37–51. https://doi.org/10.1016/j.wasman.2024.05.029.
[41] Kim M, Chul P, Kim W, Cui F. Application of data smoothing and principal component analysis to develop a parameter ranking system for the anaerobic digestion process. Chemosphere 2022;299:134444. https://doi.org/10.1016/j.chemosphere.2022.134444.
[42] Costa JC, Alves MM, Ferreira EC. Principal component analysis and quantitative image analysis to predict effects of toxics in anaerobic granular sludge. Bioresour Technol 2009;100:1180–5. https://doi.org/10.1016/j.biortech.2008.09.018.
[43] Pechaud Y, Pageot S, Goubet A, Duran Quintero C, Gillot S, Fayolle Y. Size of biological flocs in activated sludge systems: Influence of hydrodynamic parameters at different scales. J Environ Chem Eng 2021;9:105427. https://doi.org/10.1016/j.jece.2021.105427.
[44] Jin B, Lant P. Flow regime, hydrodynamics, floc size distribution and sludge properties in activated sludge bubble column, air-lift and aerated stirred reactors. Chem Eng Sci 2004;59:2379–88. https://doi.org/10.1016/j.ces.2004.01.061.
[45] Wilén B-M, Balmér P. The effect of dissolved oxygen concentration on the structure, size and size distribution of activated sludge flocs. Water Res 1999;33:391–400. https://doi.org/10.1016/S0043-1354(98)00208-5.